American Journal of Biomedical Engineering 2013, 3(6): 199-207
DOI: 10.5923/j.ajbe.20130306.09

An Efficient Algorithm for Remote Detection of Simulated Heart Rate Using Ultra-Wide Band Signals

Amjad Hashemi[1], Alireza Ahmadian[1,*], Mehran Baboli[2]

[1]Department of Biomedical Engineering and Medical Physics & Research Centre for Biomedical Technology and Robotics, RCBTR, Tehran University of Medical Sciences, Tehran, Iran
[2]Department of Electrical Engineering, University of Hawaii at Manoa, Honolulu

Abstract Ultra-wideband (UWB) signals have become attractive because of their particular advantage of having a narrow pulse width, which makes them suitable for non-invasive remote sensing of vital signals. In this paper, we present an efficient algorithm based on power spectral method applied on UWB signals for non-invasive monitoring and measurement of simulated heart rates. The objective of this study is to evaluate practical algorithms for wireless detection of the human heart rate using UWB signals in a noisy environment. To perform this, the heart rate is first simulated by our designed moving phantom with variable speed and range of motion. Then, these data were entered in the proposed simulation framework including a new multilayer UWB channe l to resemble the human body to detect accurate heart rate using an UWB transceiver with 3.2GHz of bandwidth in a noisy environment. We evaluate and compare the motion rate detection techniques based on variance, Fourier transform, wavelet transform, and power spectrum density, PSD. Experimental results show that our approach based on PSD is well adapted to detect the simulations by the motion phantom. The results prove an accuracy of 98% achieved by PSD method for detection of various periodic movements of the motion phantom. The result shows that this algorithm is capable of being used in real time applications and is promising for daily clinical use.

Keywords Ultra-wideband, Wireless Detection, Virtual Motion Phantom, Power Spectrum Density, Fourier Transform, Wavelet Transform

1. Introduction

Monitoring of patient's heart and respiration rates is frequently performed in clinical treatment programs. Most of the commonly used monitoring tools in clinical applications need to be in direct touch with the patient's body that obviates patient compliance. Recently, new technologies have been developed to remotely monitor these vital signals with wireless transmission by employing an ultra-wideband (UWB) technique as a promising candidate[1- 3].

In February 2002, Federal Communications Commission (FCC) legalized the use of UWB by releasing a set of spectral masks[4, 5]. Since then, UWB signals have found widespread use in medical applications, e.g., in the early stage detection of breast cancer[6- 8], and in wireless tracking systems[9, 10]. Because of high spatial resolution in comparison with the heart and respiration frequency, as well as the high data rate and resistance to jamming, UWB can be used for detection of heart and chest cavity movements. However, these signals have low power and they are considerably attenuated in the propagation environment. Therefore, they need robust and sophisticated algorithms for detection[3, 11, 12].

The detection of heart and respiratory rates employing UWB signals has been an active research area[13, 14]. A UWB-simulated framework based on a layered-based channel model was proposed to evaluate the effects of simulation and heart motion parameters such as the thickness of channel layers on the accuracy of heart rate measurements. Based on simulated system proposed by the authors of this paper[15], a MATLAB framework presented which simulates an environment whereby the UWB signals can be observed and evaluated at different locations of the simulated channel for wireless measurement of heart rate. Main parts of the simulated system include UWB signal generator, transmitter and receiver, as well as a new channel which models different layers of human body. The proposed system enables us to evaluate the effect of different parameters, such as thickness of channel layers and heart motion parameters on the accuracy of heart rate measurement. One of the main features of that work is employing a five layers channel model with arbitrary attenuation parameters defined by user for simulation of human body. This multi-layer channel model was used to simulate and evaluate the effects of UWB wave propagation through the human body[15, 16]. The proposed mathematical framework of the UWB channel model has

* Corresponding author:
Ahmadian@sina.tums.ac.ir (Alireza Ahmadian)
Published online at http://journal.sapub.org/ajbe

been adopted in this paper. A detection algorithm followed by real experiments was proposed to remove respiration from the data and to calculate the heart rate[17]. The main disadvantage of this algorithm was its sensitivity to the noise. Respiration was detected in the real data using an algorithm based on continuous wavelet transform[14]. Selection of the mother wavelet in this algorithm was based on the shape of the transmitted pulse; hence, it has limitations in application to the data acquired by another UWB transceiver. Another wavelet based algorithm using full wavelet packets with slow calculations was previously reported and tested on the real data[16]. A statistical algorithm to detect respiratory and heart rates has been reported previously[18, 19]. The main contribution of these studies was providing an analytical framework for the development of signal processing algorithms to estimate respiration and heart rates and corroboration of the techniques with measurements.

In this paper we have extended our previous works to become more precise and accurate in detecting the target's heart rate in an environment containing other objects without any wave absorber. Furthermore, a simulated system is proposed to compare the simulation results and those of real experiments.

2. Materials and Methods

2.1. Simulation Framework

In this section, a simulation framework to simulate the UWB system and to detect the heart rate is presented. In this simulated system the transmitter sends a Gaussian monocycle pulse with a bandwidth of 3.2GHz (Fig. 1). Antennas are exactly located in front of the target's heart to achieve minimum wave attenuation[16].

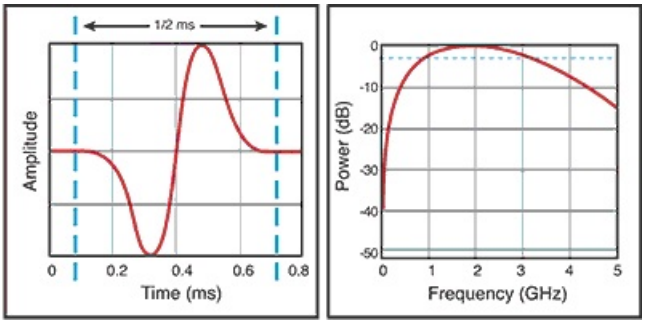

Figure 1. Gaussian monocycle pulse, Time domain and Frequency domain

The propagation channel only attenuates the signals and obviated to consider the effects of scattering and multipath propagation. The model of UWB channel is shown in Fig. 2. This UWB channel consists of five layers and the thickness of each layer can be changed. Transmission and the reflection coefficients for different layers can be calculated and to be used for the data processing and heart rate detection. Here it is assumed that waves travel only perpendicular to the planar interface between two different layers. Therefore, effects of multipath fading as a result of scattering and multipath propagation are not considered. This model is valid only for short ranges of wave propagation. Attenuation depends on the frequency of the signal which is assumed to be 3GHz[16].

Air	Fat	Muscle	Cartilage	Lung	Heart
(A)	(F)	(M)	(C)	(L)	(H)

Figure 2. Channel model

Based on the conditions proposed by Baboli[16], transmitted and received average power densities can be written as:

Transmitted power:

$$S_{av}^{t} = \left(\frac{\eta_1}{\eta_2}\left|\frac{2\eta_2}{\eta_2+\eta_1}\right|^2\right).e^{-2\alpha_2 z_2}.S_{av}^{i} \quad (1)$$

Received power:

$$S_{av}^{r} = \left(\left|\frac{\eta_2-\eta_1}{\eta_2+\eta_1}\right|^2\right).e^{-2\alpha_2 z_2}.S_{av}^{i} \quad (2)$$

where z is the layer thickness, and α and η are the attenuation constant and intrinsic impedance, respectively, as calculated in[16],

Layer	Layer	Layer	…..	Layer	Layer
1	2	3		J	j+1

Figure 3. Schematic of the multi-layer

Figure 3 shows the schematic of a multi-layer model to take into account the attenuation effects of different tissues and propagation media on UWB signal. According to such a model when different propagation layers are consecutive, the wave that passes through the first interface ($S_{av,1}^{t}$) is the incident wave for the second interface ($S_{av,2}^{t}$). Hence the transmitted power for each layer can be written as follows[20]:

$$S_{av,1}^{t} = \left(\frac{\eta_1}{\eta_2}\left|\frac{2\eta_2}{\eta_2+\eta_1}\right|^2\right).e^{-2\alpha_2 z_2}.S_{av,1}^{i} \quad (3)$$

$$S_{av,2}^{t} = \left(\frac{\eta_2}{\eta_3}\left|\frac{2\eta_3}{\eta_3+\eta_2}\right|^2\right).e^{-2\alpha_3 z_3}.S_{av,1}^{t} \quad (4)$$

$$S_{av,3}^{t} = \left(\frac{\eta_3}{\eta_4}\left|\frac{2\eta_4}{\eta_4+\eta_3}\right|^2\right).e^{-2\alpha_4 z_4}.S_{av,2}^{t} \quad (5)$$

$$\vdots$$

$$S_{av,j}^{t} = \left(\frac{\eta_j}{\eta_{j+1}}\left|\frac{2\eta_{j+1}}{\eta_{j+1}+\eta_j}\right|^2\right).e^{-2\alpha_{j+1} z_{j+1}}.S_{av,j-1}^{t} \quad (6)$$

Consequently, the total attenuation of the signal after transmitting through layer j is calculated using the next equation:

$$att_1 = \prod_{k=1}^{j}\left(\frac{\eta_k}{\eta_{k+1}}\left|\frac{2\eta_{k+1}}{\eta_{k+1}+\eta_k}\right|^2.e^{-2\alpha_{k+1} z_{k+1}}\right) \quad (7)$$

Let us assume that the wave is reflected from the (j+1)th interface. We have:

$$\mathrm{att}_2 = \frac{\eta_{j+1}-\eta_j}{\eta_{j+1}+\eta_j} \quad (8)$$

Then, the wave returns from the same path to the receiver. Attenuation in the returning path is as follows:

$$\mathrm{att}_3 = \prod_{k=1}^{j}\left(\frac{\eta_{k+1}}{\eta_k}\left|\frac{2\eta_k}{\eta_{k+1}+\eta_k}\right|^2 . e^{-2\alpha_k z_k}\right) \quad (9)$$

Finally, the total attenuation is calculated from (5) as follows:

$$\mathrm{att} = \mathrm{att}_1 \times \mathrm{att}_2 \times \mathrm{att}_3 \quad (10)$$

For simplicity, we can consider all of those calculations in decibels:

$$\mathrm{att}_1|_{dB} = \sum_{k=1}^{j}\left(\left(\frac{\eta_k}{\eta_{k+1}}\left|\frac{2\eta_{k+1}}{\eta_{k+1}+\eta_k}\right|^2 . e^{-2\alpha_{k+1} z_{k+1}}\right)|_{dB}\right) \quad (11)$$

$$\mathrm{att}_3|_{dB} = \sum_{k=1}^{j}\left(\left(\frac{\eta_{k+1}}{\eta_k}\left|\frac{2\eta_k}{\eta_{k+1}+\eta_k}\right|^2 . e^{-2\alpha_k z_k}\right)|_{dB}\right) \quad (12)$$

$$\mathrm{att}|_{dB} = \mathrm{att}_1|_{dB} + \mathrm{att}_2|_{dB} + \mathrm{att}_3|_{dB} \quad (13)$$

2.2. Experiments

Experiments are designed to verify the detection algorithm and the simulation results. Several experiments are performed, and the goal of each step was to develop and complete the simulation framework and improve the detection algorithm for detecting the heart beats.

Antennas are located near the chest cavity and both the human target and radars are covered with wave absorbing materials to restrict unwanted interferences. Under such a situation, the propagation channel only contains the human body.

Physical geometry of the propagation environment (e.g., distance between radars and the chest cavity), transmit pulses and related parameters (e.g., transmission frequency), as well as the expected heart rate are similarly chosen in the simulation (Fig. 4).

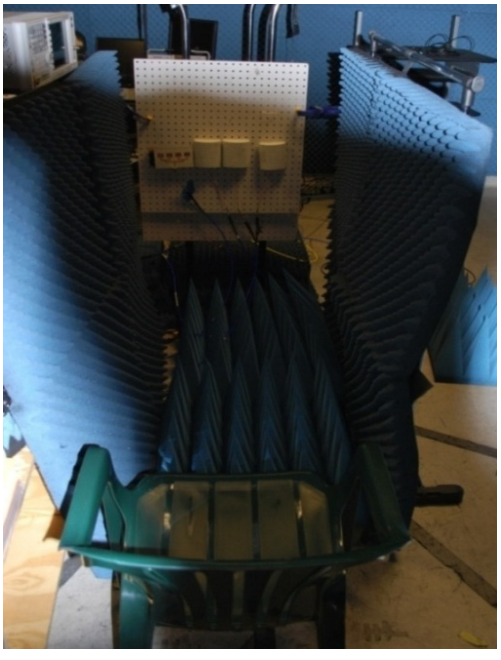

Figure 4. Measurement setup for controlled environment

The experiments are performed using the Time Domain PulsON P220 Evaluation Kit. Its specification and the parameters of the transceiver are shown in Table 1.

Table 1. Specification and the parameters of transceiver

PRF(Pulse Repetition Frequency)	9.6 MHz
Center frequency	4.7 GHz
Band width	3.2GHz
Power consumption	5.7 W
Raw data rate	9.6 Mbps

For full control of target frequency, a virtual thorax motion phantom with the capability of setting the frequency and movement range was built and used in the experiment. The frequency and range of motion were controlled using an ATMEGA32 microcontroller. For setting the initial position of the movement, the system uses an infra-red sensor. The phantom is shown in Fig. 5.

Figure 5. A virtual thorax motion phantom

2.3. Methods

The heart layer, which is the last layer in this model, is considered as the only moveable layer. Here it is assumed that heart has linear one-dimensional movement which leads to generates linear Doppler.

In this study we evaluate techniques based on variance, Fourier transform, wavelet transform and power spectral density, PSD for phantom motion rate detection. In all techniques body movement cancellation and removing background clutter is the same.

The five steps of algorithm to detect heart rate are described in the following as shown in Fig 6:

(1) Each received waveform is recorded in one row of a matrix called the received matrix, R.

(2) For removing the body movement, the cross correlation between each row of matrix R, (each received waveform) and the first row, which is considered the base waveform in the time domain, is calculated. Then, each row is circularly shifted to the point where the amount of its

corresponding cross correlation is maximized.

(3) The motion filter is applied on the matrix. This filter calculates the average of each column and subtracts it from each sample of that column (7),

$$R_m(i.j) = R(i,j) - \frac{1}{N}\sum_{l=1}^{N} R(i,j) \quad (14)$$

where R is the received matrix and N is the total number of rows of matrix R.

(4) After applying the motion filter, the static background is removed and only the dynamic part of the channel data remains. This part consists of data related to the heart beat of the target. The goal of this step is to find a column from matrix R_m, in which the heart motion data is appeared. It is shown in[14] that the total energy of the samples for each column is maximized in a column, which contains motion data.

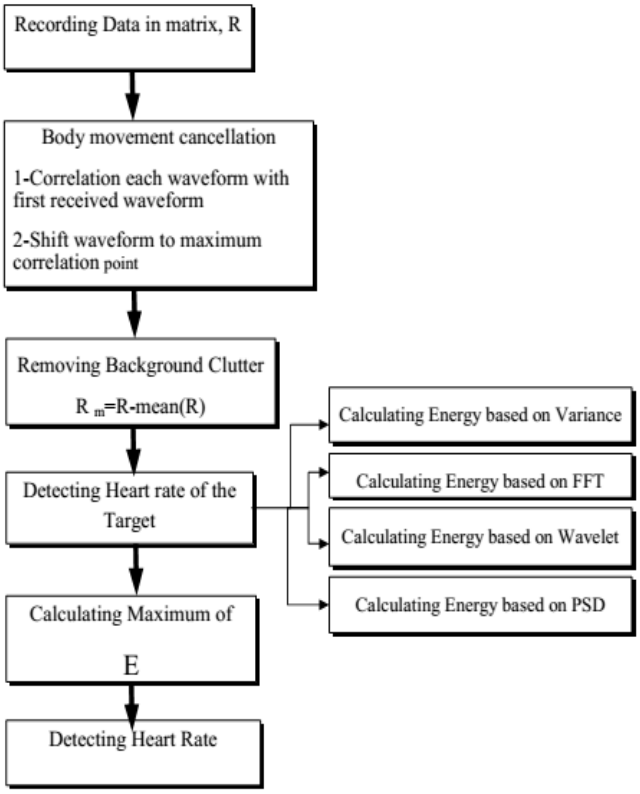

Figure 6. Block diagram of the proposed algorithm

Various methods to evaluate

(a) Variance method: To perform this, the variance of all columns was calculated, and the column with maximum variance is selected as the reference line called t_p.

(b) Fourier transform method: Discrete Fourier Transform (DFT) of matrix R was calculated and recorded in matrix R_{FFT}. In the frequency domain, for finding the column that has the maximum energy, the proportion of peaks $R_{FFT}(i,j)^2$ to the total energy of signals in each column was calculated by (15) and recorded in array E_{fft},

$$E_{fft}(j) = \frac{\max(R_{FFT}(i,j)^2)}{\sum_{l=0}^{i=L} R_{FFT}(i,j)^2} \quad (15)$$

Where j is the column index, i is the row index, and L is the number of rows in matrix R_{FFT}. The column, in which E has the maximum value, is the target point and is called t_p. The frequency of the peak in the frequency spectrum of column t_p is the frequency of motion.

(c) Discrete wavelet transform: The procedure of multi-resolution decomposition of a signal R[n] is implemented using a complementary low-pass/high-pass filtering followed by down-sampling by 2. Each step of this scheme consists of two digital filters and two down samplers by 2. The outputs of the high-pass filters are details and those of the low-pass filters are approximations. The wavelet transform, which is used in this paper for respiration rate calculations, is as follows:

$$(T_{m,n}) = \int_{-\infty}^{+\infty} R(t) \frac{1}{a_0^{m/2}} \psi(a_0^{-m} t - nb_0) dt \quad (16)$$

where ψ is the mother wavelet, n is the translation, m is the dilation, a_0 is the dilation step parameter, and b_0 is the location parameter. The energy of the wavelet is as follows:

$$E_m = \sum_{n=0}^{2^{M-m}} (T_{m,n})^2 \quad (17)$$

In this study the Daubechies 8 wavelet filter was chosen as the mother wavelet. Wavelet transform was applied on all of the columns of matrix R. Then, the energy of all of the frequency intervals is calculated and their maximum is saved in an array, $E_{wavelet}$. The column, in which $E_{wavelet}$ has its maximum value, presents the location of the motion that is occurred.

(d) Power spectrum density (PSD): The main step in the detection algorithm is to find the column that contains motion data. In real conditions, applying the variance method does not give a correct answer when the experiment is being repeated. The reason is that the received waveform consists of many multipaths from different objects, which are correlated to each other. Moreover, the noise affected data more than the situation when the wave absorber was used. These problems yields maximizing of the variance at false points; hence, we have improved the signal processing algorithm in[18, 19] and proposed an algorithm based on the distributed energy in the frequency domain and spectral analysis of the data. The details of the algorithm is described as follows:

After application of the motion filter, PSD is applied on each column and the frequency spectrum of each column is recorded in matrix R_{PSD}. This feature computes the PSD of each column through the Fourier transform of the autocorrelation of each column. PSD illustrates how the power of a signal is distributed over the different frequencies. The spectral representation is a very useful device for describing stationary random processes in the frequency domain. The formula is as follows:

$$R_{PSD} = \frac{|FFT\{R_{xx}^n\}|_{f=Mf}}{N} \quad (18)$$

where R_{xx}^n is the autocorrelation function of the n_{th} column.

For finding the phantom motion, the column that has the maximum energy has to be detected. The proportion of the PSD signal in each column to the total PSD of signals was calculated using (19) and recorded in array $E_{psd,}$

$$E_{psd}(j) = \frac{\max(R_{PSD}(i,j)^2)}{\sum_{I=0}^{i=L} R_{PSD}(i,j)^2} \quad (19)$$

where j,i, and L are the column index, row index, and number of rows in matrix R_{PSD}, respectively. The column, in which E_{psd} has the maximum value, is the target point and is called t_p. By applying Fourier transform on the t_p column, the frequency of motion was detected. The complete flowchart of the algorithm is shown in Fig. 6.

3. Results

In order to evaluate the robustness of the proposed algorithm to detect the heart rate, experiments were performed with six different subjects in different propagation and noisy environments. The results were obtained in an environment that contains other objects, which act as reflectors. Data had pulse periods equal to 100 and 200 millisecond.

Results for the case of pulse periods equal to 100 and 200 ms are shown in Figs. 7 and 8, respectively. The motion rate of phantom is detected with a maximum error of 2.2%. The results associated with other subjects are shown in Table 2.

Table 2. Specification and the parameters of transceiver

Subject	Pulse period	Motion Rate	PSD Method	Variance Method	FFT Method	Wavelet Method
1	100	60	60.24	63.6	61.2	58.2
2	100	90	89.1	87.4	88.14	87.4
3	100	120	121	113.4	122.4	113.4
4	200	60	58	64.8	63.6	62.4
5	200	90	88.8	92.1	92.1	88.8
6	200	120	112.2	104	112.2	109.2

To evaluate our algorithm in a noisy environment, we added white Gaussian noise to the signal. The phantom motion rate was undetectable with SNR=10 and less. Our algorithm based on the PSD algorithm in a noisy environment with SNR=15 has the same result as that obtained in a clean environment. Figures 9 and 10 show noisy signals.

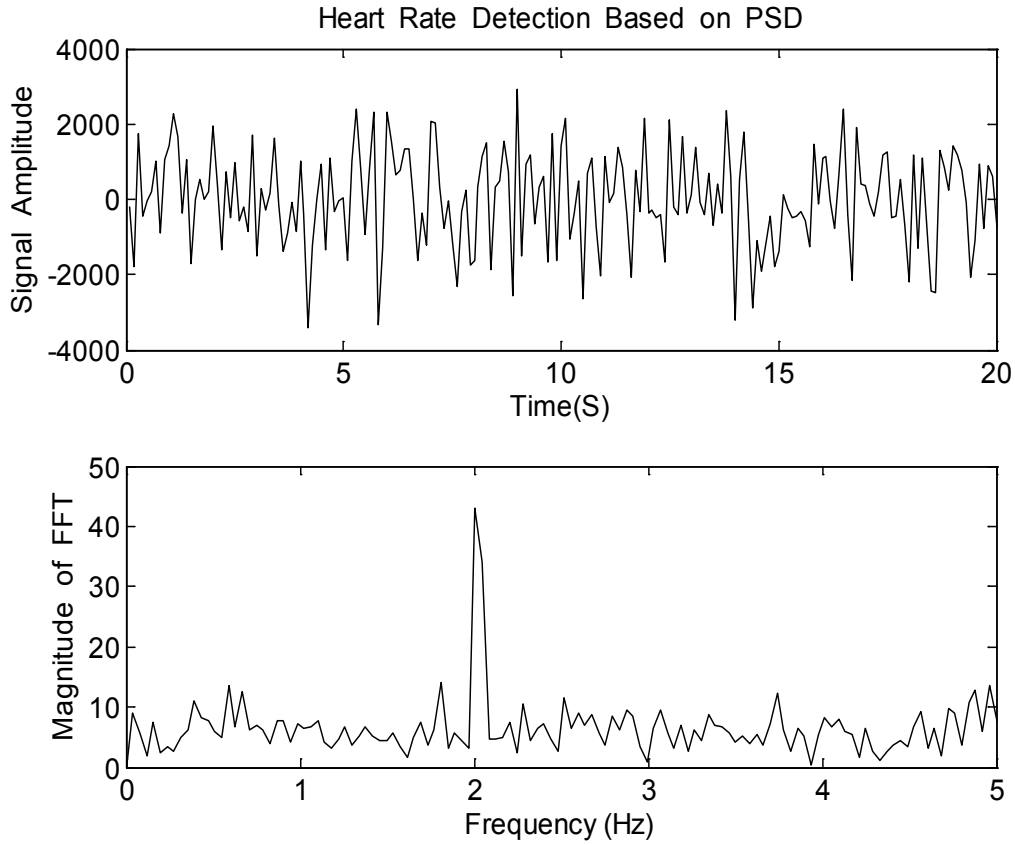

Figure 7. Simulation experimental results of controlled conditions in the frequency and time domain with a pulse period of 100 ms

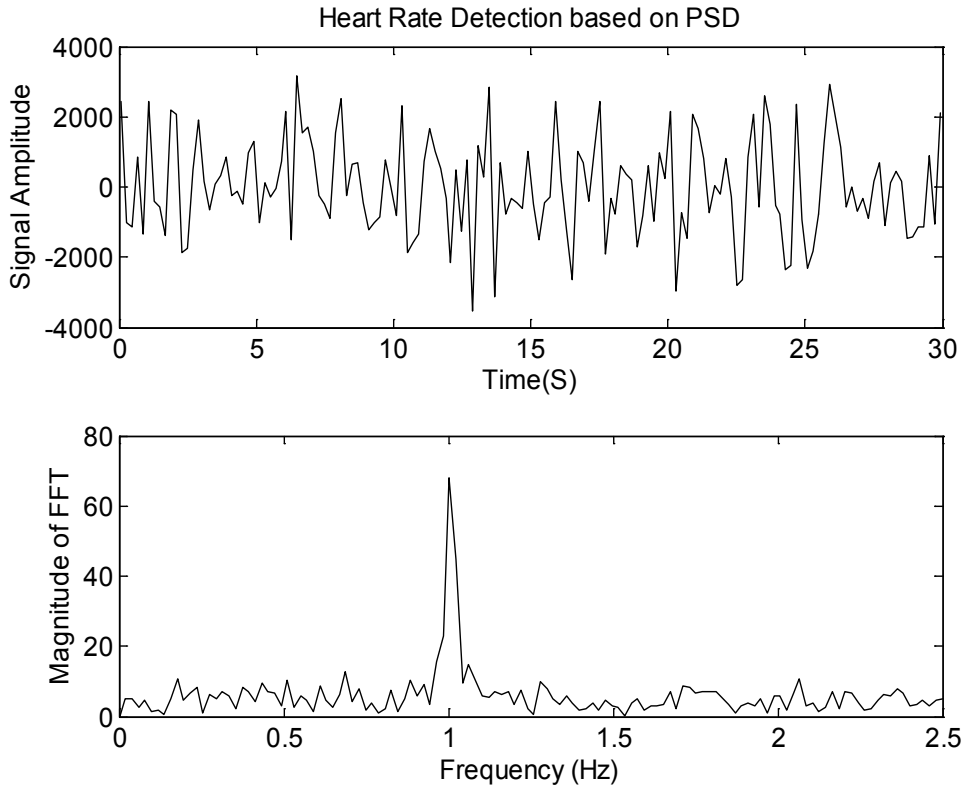

Figure 8. Simulation experimental results of controlled conditions in the frequency and time domain with a pulse period of 200 ms

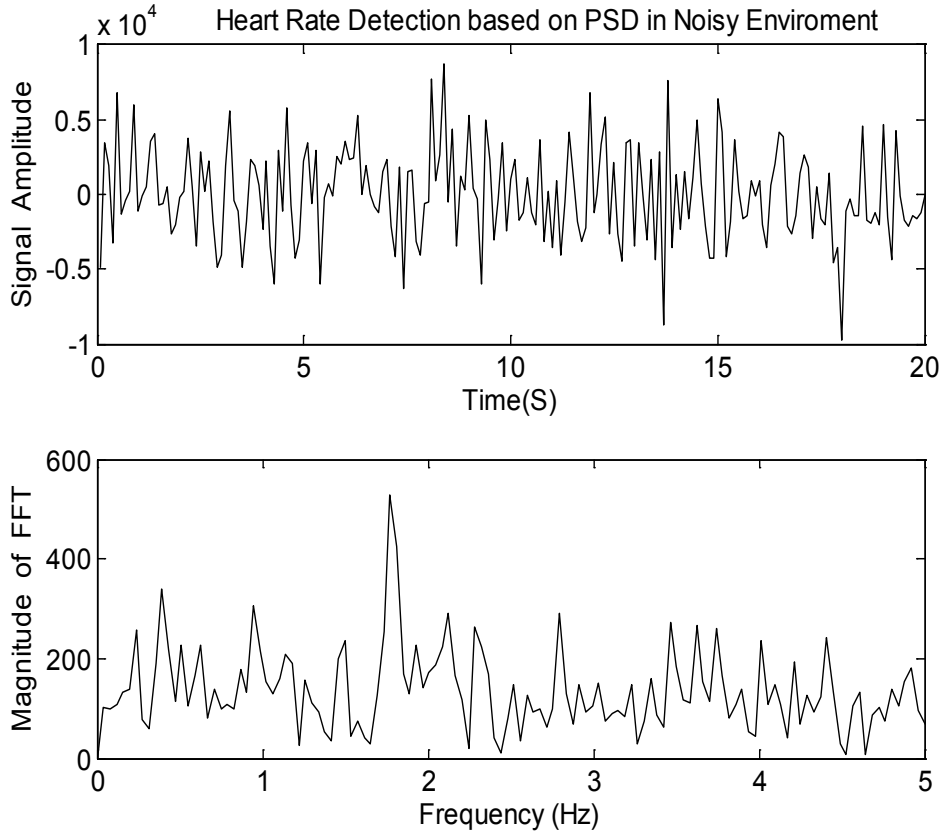

Figure 9. Simulation experimental results of controlled conditions in the frequency and time domain with a pulse period of 100 ms in a noisy environment (SNR=15)

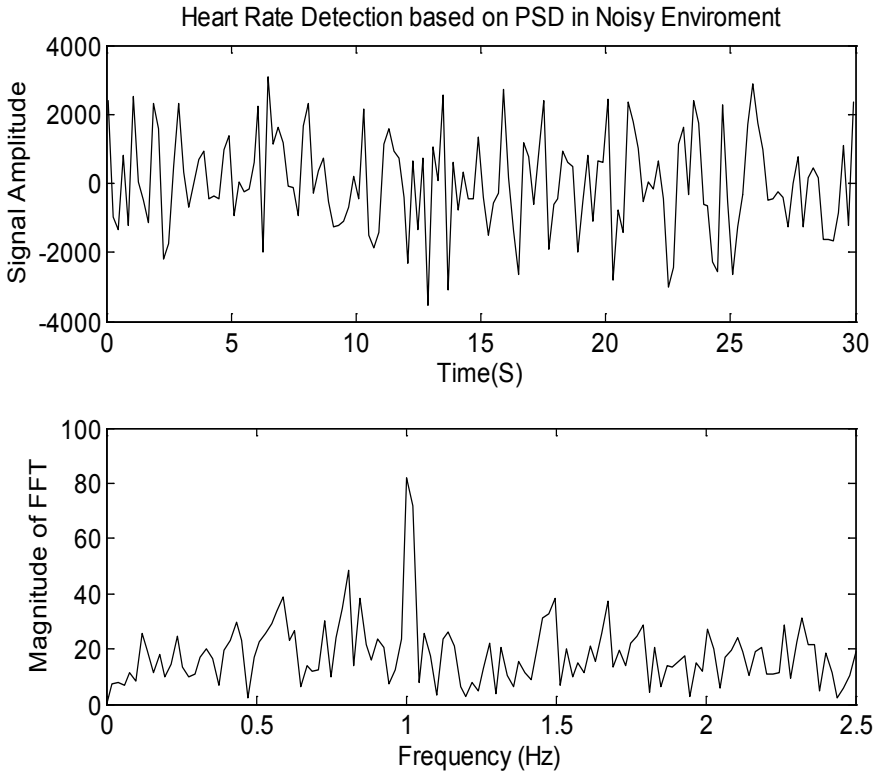

Figure 10. Simulation experimental results of controlled conditions in the frequency and time domain with a pulse period of 200 ms in a noisy environment (SNR=15)

4. Conclusions

In this paper we have proposed a UWB-based monitoring technique for non-invasive detection of motion phantom rates for subjects located within a few meters of the radar. A flexible UWB framework is presented, which simulates an environment in which UWB signals can be observed and evaluated for wireless measurement of motion phantom rates and diagnoses of heart arrhythmias.

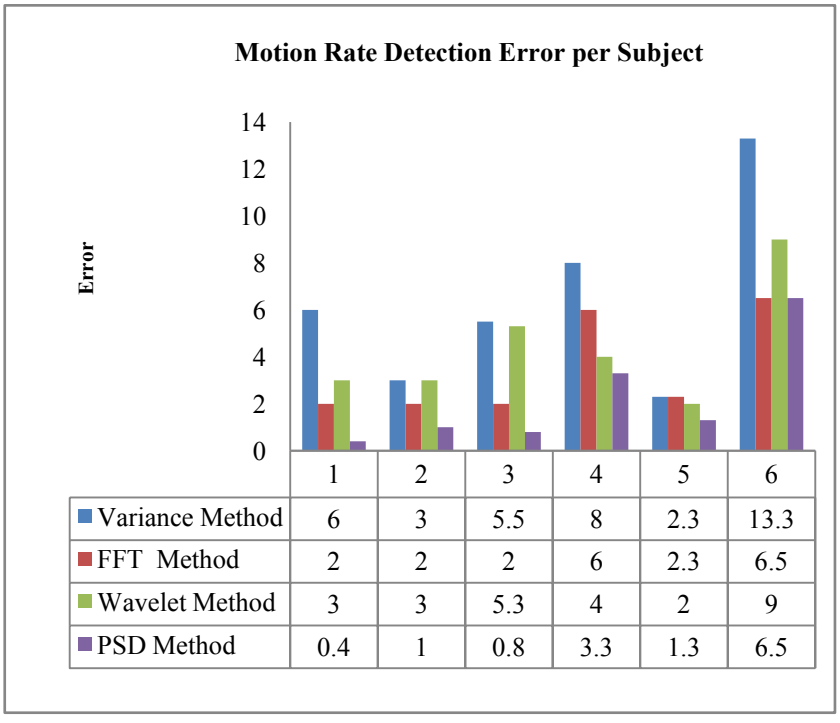

	1	2	3	4	5	6
Variance Method	6	3	5.5	8	2.3	13.3
FFT Method	2	2	2	6	2.3	6.5
Wavelet Method	3	3	5.3	4	2	9
PSD Method	0.4	1	0.8	3.3	1.3	6.5

Figure 11. Error calculated in variance, FFT, wavelet, and PSD algorithms in six subjects

In this study, some well-known methods based on variance, Fourier transform, wavelet transform and PSD for detection of phantom motion rate were applied. In all techniques body movement cancellation, removing background clutter was same.

By employing cross correlation between each row of data matrix R and the first row of the matrix R, body movement was calculated, and then circularly shifted to the point where the amount of its corresponding cross correlation is maximized, all data were synchronized.

Background clutter was omitted by subtracting the average of each column from all samples in that column.

In the proposed algorithm, after body movement cancellation and background clutter removal, an algorithm based on PSD in frequency domain for heart rate detection is applied. The results of PSD algorithm in this step proved an accuracy of 97.8% in simulated data. Figure 11 shows error in variance, FFT, wavelet, and PSD methods. Error averages obtained in these algorithms are 6.35%, 3.46%, 4.4%, and 2.2%, respectively. This result shows that a motion phantom algorithm based on PSD performs the best results.

This framework can be used as a basis to design/evaluate practical UWB systems with proper parameters for motion phantom rate detection. This provides us with the expected results of employing such a system in real situations. The new efficient algorithm proposed here can be used to accurately estimate the motion phantom rate in a noisy environment. The presented framework is potentially applicable in remote detection of abnormalities in respiratory and heart rates.

ACKNOWLEDGEMENTS

This research was supported by Tehran University of Medical Sciences and Institute for Advanced Medical Technologies (IAMT), Research Centre for Biomedical Technology and Robotics.

REFERENCES

[1] E,Pancera. X, Li. M , Jalilvand. T, Zwick. W, Wiesbeck. “UWB medical diagnostic: in-body transmission modeling and applications”. in Antennas and Propagation (EUCAP), Proceedings of the 5th European Conference on. IEEE. 2011.

[2] A, Taparugssanagorn. A, Rabbachin. J, Saloranta. J, Iinatti, “A review of channel modelling for wireless body area network in wireless medical communications”. 2008.

[3] G, Varotto and E.M. Staderini, “On the UWB medical radars working principles”. International Journal of Ultra Wideband Communications and Systems, 2(2): p. 83-93, 2011.

[4] G, Breed. “A summary of FCC rules for ultra wideband communications. High Frequency Electronics”. 4(1): p. 42-44. 2005.

[5] S, Hanna. “Regulations and standards for wireless medical applications”. in Proceedings of the 3rd international symposium on medical information and communication technology. 2009.

[6] A.M, Abbosh,., M.E. Bialkowski, and S. Crozier. “Investigations into optimum characteristics for the coupling medium in UWB breast cancer imaging systems”. in Antennas and Propagation Society International Symposium, IEEE. 2008.

[7] M, Klemm. I,Craddock. J, Leendertz. A, Preece. R, Benjamin. “Experimental and clinical results of breast cancer detection using UWB microwave radar. in Antennas and Propagation” Society International Symposium, 2008.

[8] M , Guardiola. S, Capdevila.S,Blanch. J, Romeu L, Jofre. “UWB high-contrast robust tomographic imaging for medical applications”. IEEE International Conference in Electromagnetics in Advanced Applications, 2009.

[9] W, Zhiguo. Xi, L and F. Yuanchun. “Moving target position with through-wall radar”. IEEE International Conference in Radar, 2006.

[10] S. Ergut, R. R. Rao, O. Dural, and Z. Sahinoglu, "Localization via TDOA in a UWB Sensor Network using Neural Networks," IEEE International Conference in Communicati ons, pp. 2398-2403, 2008.

[11] M, Jalilvand, Li, X. T, Zwick,W, Wiesbeck. E Pancera. “Hemorrhagic stroke detection via UWB medical imaging”. IEEE Proceedings of the 5th European Conference in Antennas and Propagation, 2011.

[12] G.A ,Zito, E.M. Staderini, and S. Pisa, “A twin spiral planar antenna for UWB medical radars”. International Journal of Antennas and Propagation, 2013.

[13] G. Ossberger, T. Buchegger, E. Schimback, A. Stelzer, and R. Weigel, "Non-invasive respiratory movement detection and monitoring of hidden humans using ultra wideband pulse radar," International Workshop in Ultra Wideband Systems, pp. 395-399, 2004.

[14] S. Venkatesh, C. R. Anderson, N. V. Rivera, and R. M. Buehrer, "Implementation and analysis of respiration-rate estimation using impulse-based UWB," IEEE Conference in Military Communications, MILCOM, pp. 3314-3320. 2005.

[15] M. Baboli, A. Sharafi, A. Ahmadian, and S. KarimiFard, "A framework for simulation of UWB system for heart rate detection," International Conference in Biomedical and Pharmaceutical Engineering, pp. 1-5. 2009.

[16] M. Baboli, S. A. Ghorashi, N. Saniei, and A. Ahmadian, "A new wavelet based algorithm for estimating respiratory motion rate using UWB radar". International Conference in Biomedical and Pharmaceutical Engineering, pp. 1-3. 2009.

[17] S. N. Pavlov and S. V. Samkov, "Algorithm of signal processing in ultra-wideband radar designed for remote measuring parameters of patient's cardiac activity," Second International Workshop in Ultrawideband and Ultrashort Impulse Signals, pp. 205-207, 2004.

[18] M. Baboli, A. Sharafi, A. Ahmadian, and M. S. Nambakhsh, "An accurate and robust algorithm for detection of heart and respiration rates using an impulse based UWB signal," International Conference in Biomedical and Pharmaceutical Engineering, pp. 1-4. 2009.

[19] Sharafi, A., M. Baboli, and M. Eshghi. A new algorithm for

detection motion rate based on energy in frequency domain using UWB signals. International Conference in Bioinformatics and Biomedical Engineering (iCBBE), 2010.

[20] C, Bilich, "UWB radars for Bio-Medical Sensing: Attenuation Model for Wave Propagation in the body at 4GHz". 2006.